Autti, Samuli; Bunkov, Yu.M.; Eltsov, Vladimir; Heikkinen, P.J.; Hosio, J.J.; Hunger, P.; Krusius, M.; Volovik, Grigory

Self-trapping of magnon Bose-Einstein Condensates in the ground state and on excited levels: from harmonic to box cofinement

Published in:
Physical Review Letters

DOI:
10.1103/PhysRevLett.108.145303

Published: 01/01/2012

Document Version
Publisher's PDF, also known as Version of record

Please cite the original version:
Autti, S., Bunkov, Y. M., Eltsov, V. B., Heikkinen, P. J., Hosio, J. J., Hunger, P., ... Volovik, G. E. (2012). Self-trapping of magnon Bose-Einstein Condensates in the ground state and on excited levels: from harmonic to box cofinement. Physical Review Letters, 108(14), 1-5. [145303]. https://doi.org/10.1103/PhysRevLett.108.145303

Self-Trapping of Magnon Bose-Einstein Condensates in the Ground State and on Excited Levels: From Harmonic to Box Confinement

S. Autti,[1] Yu. M. Bunkov,[2] V. B. Eltsov,[1] P. J. Heikkinen,[1] J. J. Hosio,[1] P. Hunger,[2] M. Krusius,[1] and G. E. Volovik[1,3]

[1]*Low Temperature Laboratory, School of Science, Aalto University, Finland*

[2]*Institute Néel, CNRS, Grenoble, France*

[3]*L.D. Landau Institute for Theoretical Physics, Moscow, Russia*

(Received 14 November 2011; published 3 April 2012)

Long-lived coherent spin precession of ^{3}He-B at low temperatures around $0.2T_c$ is a manifestation of Bose-Einstein condensation of spin-wave excitations or magnons in a magnetic trap which is formed by the order-parameter texture and can be manipulated experimentally. When the number of magnons increases, the orbital texture reorients under the influence of the spin-orbit interaction and the profile of the trap gradually changes from harmonic to a square well, with walls almost impenetrable to magnons. This is the first experimental example of Bose condensation in a box. By selective rf pumping the trap can be populated with a ground-state condensate or one at any of the excited energy levels. In the latter case the ground state is simultaneously populated by relaxation from the exited level, forming a system of two coexisting condensates.

DOI: 10.1103/PhysRevLett.108.145303 PACS numbers: 67.30.er, 03.70.+k, 05.30.Rt, 11.10.Lm

During the last few years increasing efforts have been invested in the investigation of Bose-Einstein condensation (BEC) of nonconserved bosons, such as magnons [1,2], photons [3], and exciton-polaritons [4]. BEC of quasiparticles and other particlelike excitations is a special case since in thermal equilibrium their chemical potential vanishes. Formally BEC requires conservation of the particle number, but condensation can still be extended to systems with weakly violated conservation. For sufficiently long-lived excitations, the nonzero chemical potential is well defined and condensation becomes possible. The loss of (quasi)particles owing to their decay does not violate the coherence and can be compensated by pumping. Magnons in superfluid ^{3}He-B satisfy this condition and condensation there is observed as spontaneous long-lived coherent precession of spins which is accompanied by various phenomena of spin superfluidity [5]. Different types of magnon BEC have been identified in ^{3}He-B, starting from the so-called "Homogeneously Precessing Domain" (HPD), which represents a bulk condensate state.

In ^{3}He-B at low temperatures the HPD state becomes unstable owing to parametric creation of spin waves, but another type of coherent long-lived NMR signal with several orders of magnitude smaller amplitude was discovered in this regime [6]. The mode was ascribed to magnon condensation in a magnetic trap formed in a weakly inhomogeneous order-parameter distribution or texture [1], but the piecemeal information obtained with pulsed and cw NMR measurement has been confusing. Here we report the first measurements with full experimental control of the order-parameter texture which produces the 3D trap. We find that when the number of magnons increases the profile of the trap changes from harmonic to boxlike. The pressure of the multimagnon wave function opens a "cavity" in a way similar to the electron bubble in liquid helium. In quantum field theory such self localization of a bosonic field is known as a Q-ball [7]. This texture-free cavity can be filled by a magnon condensate on any energy level of the trap. For cold atoms in an optical trap, the formation of a non-ground-state condensate has been discussed [8,9], but not yet realized. Of great practical importance is the fact that these magnon condensates can be used to probe the quantum vacuum state of ^{3}He-B in the limit $T \to 0$ [10], where most conventional measuring signals become insensitive.

Magnon condensation.—There are two approaches to the thermodynamics of atomic systems: one can fix the particle number $\mathcal{N}$ or the chemical potential μ. For magnon condensation, this corresponds to different experimental situations: to pulsed or continuous wave (cw) NMR, respectively. In free precession after the tipping pulse, the number of magnons pumped into the trap is conserved (if losses are neglected). This corresponds to fixed $\mathcal{N}$, when the system itself chooses the global frequency of coherent precession (= the magnon chemical potential μ [5]). The opposite case is cw NMR, when a small rf field is continuously applied to compensate for the losses. The frequency of precession ω is then that of the rf field $\omega_{\rm rf}$, the chemical potential is $\mu \equiv \omega = \omega_{\rm rf}$, and the number of magnons adjusts itself to this frequency, to match the resonance condition.

A cylindrically symmetric trap for magnons is schematically shown in Fig. 1. It is realized in a long cylindrical sample container with radius $R_s = 3$ mm in an axially oriented magnetic field (the experimental setup is described in Ref. [11]). The axial confinement potential $U_{\parallel}(z) = \omega_L(z)$, where $\omega_L(z) = \gamma H(z)$ is the local Larmor frequency, is produced by a small pinch coil, which

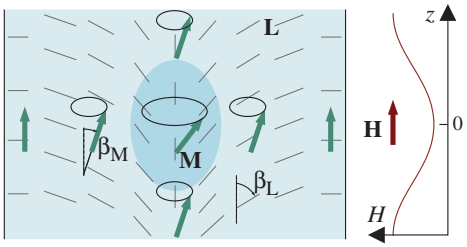

FIG. 1 (color). A sketch of the trapping potential Eq. (2) which is formed in the cylindrically symmetric "flare-out" texture of the orbital anisotropy axis **L** (thin lines) in a shallow minimum of the vertical magnetic field **H** (right). The arrows represent the magnetization **M**, which precesses coherently with constant phase angle in the condensate droplet (dark blue), in spite of the inhomogeneity in the texture and in the magnetic field.

creates a shallow minimum in the magnetic field. The radial confinement comes from the spin-orbit interaction with the texture of the orbital angular momentum **L** of Cooper pairs [5]:

$$F_{\rm so} = \frac{4\Omega_L^2}{5\omega_L}\sin^2\frac{\beta_L(r)}{2}|\Psi|^2, \qquad (1)$$

where Ψ is the wave function of the magnon condensate, Ω_L is the Leggett frequency characterizing the strength of the spin-orbit coupling, and β_L the polar angle of **L**. The trapping potential is then given as

$$U(\mathbf{r}) = U_{\parallel}(z) + U_{\perp}(r) = \omega_L(z) + \frac{4\Omega_L^2}{5\omega_L}\sin^2\frac{\beta_L(r)}{2}. \qquad (2)$$

On the side wall of the cylinder **L** is oriented normal to the wall, while on the cylinder axis **L** $\parallel$ **H**. Close to the axis β_L remains small and varies linearly with distance r. Here the potential $U(\mathbf{r})$ reduces to that of a harmonic trap, as used for the confinement of dilute Bose gases [12],

$$U(\mathbf{r}) = U(0) + \frac{m_M}{2}(\omega_z^2 z^2 + \omega_r^2 r^2), \qquad (3)$$

where m_M is the magnon mass. The low-amplitude standing spin waves have the conventional spectrum

$$\omega_{mn} = \omega_L(0) + \omega_r(m+1) + \omega_z(n+1/2), \qquad (4)$$

where $\omega_L(0) = \omega_L(z=0)$ is the Larmor frequency at the bottom of the well, which corresponds to the center of the trap in Fig. 1. The axial oscillator frequency ω_z is adjusted by changing the current in the pinch coil, while the radial frequency ω_r can be controlled by rotating the sample, since adding vortex-free superfluid flow or rectilinear vortex lines modifies the flareout texture. Let us consider the condensates which form when we start filling magnons to one of the levels (m, n) in Eq. (4).

Ground-state condensate.—When the number of magnons $\mathcal{N}$ in the ground-state (0, 0) increases, they exert an orienting effect on the **L** texture via the spin-orbit interaction in Eq. (1), which favors **L** $\parallel$ **H**. As a result at large $\mathcal{N}$ the harmonic trap transforms to a box with $\beta_L \approx 0$ within which magnons are localized. This effect is demonstrated in Fig. 2 with self-consistent calculations of the **L**-texture and of the magnon condensate wave function Ψ in the axially symmetric and z-homogeneous geometry. Rapid flattening of the texture and self-trapping of the wave function is seen to result. At large $\mathcal{N}$ the radius of localization approaches the asymptote

$$R(\mathcal{N}) \sim a_r(\mathcal{N}/\mathcal{N}_c)^p, \qquad \mathcal{N} \gg \mathcal{N}_c, \qquad (5)$$

where a_r is the harmonic oscillator length in the original radial trap (at $\mathcal{N} \ll \mathcal{N}_c$), $\mathcal{N}_c$ is the characteristic number at which the scaling starts, and $p \approx 0.2$. As in the case of the electron bubble, R is determined by a balance between the magnon zero-point energy and the surface energy of the condensate bubble. For the 2D radial texture the total energy is

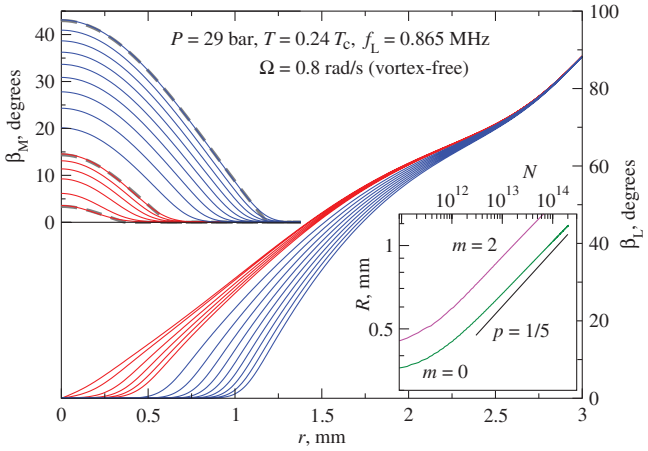

FIG. 2 (color). Numerical calculations of the magnon wave function and the order-parameter texture for multimagnon bubbles. The deflection angles of the magnetization, β_M, and of the orbital anisotropy axis, β_L, are plotted as a function of radius for different populations $\mathcal{N}$ of the ground-state, $m = n = 0$. $\mathcal{N}$ increases from bottom to top in the β_M plot and from left to right in the plot of β_L. The red curves correspond to the experimental regime in Fig. 3 (starting with $M_\perp/M_{\rm HPD} = 5 \times 10^{-4}$ and then continuing from 10^{-3} to 5×10^{-3} with a step of 10^{-3}). The blue curves illustrate extrapolations to the asymptotic regime $f \to f_L(0)$ ($M_\perp/M_{\rm HPD}$ varies from 10^{-2} to 5×10^{-2} with a step of 5×10^{-3}). When the magnon occupation increases, the magnon wave function suppresses the orbital texture β_L and the potential well transforms towards a box with impenetrable walls. Fits to the wave function of the condensate in a box are shown with broken lines in the β_M plot. The effective radius of the box obtained from such fits is shown in the *inset* as a function of $\mathcal{N}$. The slope from Eq. (5) with $p = 1/5$ is shown for comparison. Calculations for the excited radial states (ignoring relaxation to the ground state) present a similar picture. The difference is that the wave function (and thus β_M) crosses zero an appropriate number of times and the radius of localization is larger than in the ground state, as shown in the inset for $m = 2$. The reason is the larger amplitude of zero-point motion in Eq. (6), so that from (5) we have $R_{2,0}/R_{0,0} = (\lambda_2/\lambda_0)^{1/5}$.

$$E(R) = \mathcal{N}\frac{\hbar^2\lambda_m^2}{2m_M R^2} + 2\pi R\sigma(R). \quad (6)$$

The first term on the right-hand side is the kinetic energy of $\mathcal{N}$ magnons in a cylindrical box, where λ_m is the mth root of the Bessel function. The second term is the surface energy with the surface tension σ which depends on R due to the flexibility of the texture. Our numerical simulations give $\sigma(R) \propto R^2$, and minimization of Eq. (6) with respect to R gives for the box radius Eq. (5) with $p \approx 1/5$.

Incidentally, for an atomic condensate with repulsive interparticle interactions, where $\mathcal{N} \gg \mathcal{N}_c$ is possible, the exponent in Eq. (5) is also $p = 1/5$ in the Thomas-Fermi limit [12]. However, owing to different scenarios of condensate formation the dependence of the frequency shift on $\mathcal{N}$ differs from the behavior of the analogous quantity in an atomic condensate; i.e., the chemical potential $\mu(\mathcal{N})$ is of the form

$$\omega - \omega_L(0) \sim \omega_r(\mathcal{N}/\mathcal{N}_c)^{-2/5}, \qquad \text{magnon BEC}, \quad (7)$$

$$\mu - U(0) \approx \omega_r(\mathcal{N}/\mathcal{N}_c)^{2/5}, \qquad \text{atomic BEC}. \quad (8)$$

In contrast to the atomic condensate, in the magnon condensate $d\omega/d\mathcal{N} < 0$. When the magnon condensate is growing, its frequency ω decreases, approaching the Larmor frequency ω_L asymptotically. This determines the way in which the magnon condensate is grown in a cw NMR experiment (Fig. 3). Magnons are created when the frequency ω of the applied rf field is swept down and crosses the ground-state level ω_{00}. With increasing $\mathcal{N}$, the potential well becomes wider radially and the energy of the trapped state decreases, finally approaching the scaling regime. Assuming that $\sigma(R) \propto R^2$ and taking into account that $\mathcal{N} = \int d^2r|\Psi|^2$ and thus $|\Psi| \sim \mathcal{N}^{1/2}/R$, one obtains for the transverse magnetization $M_\perp \propto \int d^2r|\Psi| \propto \mathcal{N}^{1/2}R \propto R^{7/2} \propto (f - f_L(0))^{-7/4}$. This agrees with the exponent -1.75 obtained in numerical simulations and in the experiment (Fig. 3, inset).

Non-ground-state condensates.—In Fig. 4 three examples of NMR spectra are shown which illustrate the magnon energy levels (m, n) in Eq. (4) under external control of the radial and axial oscillator frequencies. Here ω_r is changed by adjusting the rotation velocity Ω in the vortex-free Landau state, where the velocity of the superfluid fraction is $v_s = 0$ (in a frame fixed in the laboratory). The azimuthally flowing superfluid counterflow velocity $v_n - v_s = |\mathbf{\Omega} \times \mathbf{r}|$ modifies the $\mathbf{L}$-texture [13], making the trap steeper in the radial direction. This increases the radial frequency ω_r and the spectral distance between the radial modes. Similarly, on increasing the depth of the minimum in the field $\mathbf{H}$ the distance between the axial modes increases.

The many exited levels in Fig. 4 represent coherently precessing states with similar nonlinear population characteristics as the ground state in Fig. 3: they are

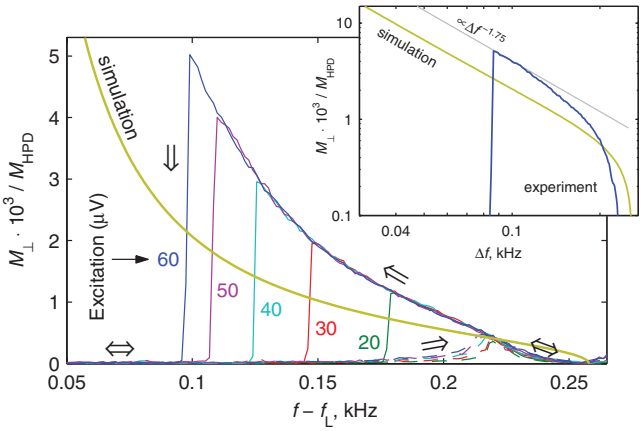

FIG. 3 (color). Formation of the magnon condensate in the ground state of the trap in Fig. 1 in cw NMR measurement. The condensate magnetization $M_\perp$ precessing in the transverse plane is plotted on the vertical axis, normalized to that when the *homogeneously precessing domain* (HPD) fills the volume within the detector coil [23]. The arrows indicate the sweep direction of the applied rf frequency $f = \omega/(2\pi)$. $M_\perp$ grows when the frequency is swept down. Only a tiny response is obtained on sweeping in the opposite direction. During the downward frequency sweep the condensate is destroyed (vertical lines), when energy dissipation exceeds the rf pumping. This point depends on the applied rf excitation amplitude, marked at each vertical line. The lower green line represents the result of calculations from Fig. 2. These calculations have no fitting parameters: the vertical difference from the measurements can be attributed to the experimental uncertainty in determining the normalization for $M_\perp$. Inset: The experimental curve measured with the largest excitation and compared to the numerical curve from the main panel, replotted with logarithmic axes to demonstrate the asymptotic limit for large magnon numbers: $M_\perp \propto [f - f_L(0)]^{-1.75}$, which corresponds to the condensate in a box.

condensates. This is a new phenomenon which becomes possible when $d\mu/d\mathcal{N} < 0$: The condensate in the state (m, n) starts to grow when the rf frequency (and thus the chemical potential) is swept down and crosses the level $\omega_{mn}(0)$ from above. During further sweeping of μ the excited state eventually collapses due to relaxation to the ground state. If the downward frequency sweep is continued further, the same behavior is repeated when the next lower excited level starts to be populated. For repulsive atomic condensates $d\mu/d\mathcal{N} > 0$ and stable non-ground-state populations cannot be formed in this way [8]. For attractive atomic condensates $d\mu/d\mathcal{N} < 0$ and in principle the present approach might then become possible.

The condensate on a level (m, n) can be maintained in steady state only if the proper chemical potential is applied, i.e., under continuous pumping at $\omega_{mn}(\mathcal{N})$. After switching off the pumping, the condensate is manifested as long-lived ringing of the free induction signal. In Fig. 5 the decay of the induction signal has been recorded, showing two coexisting condensates: at the excited (2, 0) level, where the magnons were initially pumped, and in the

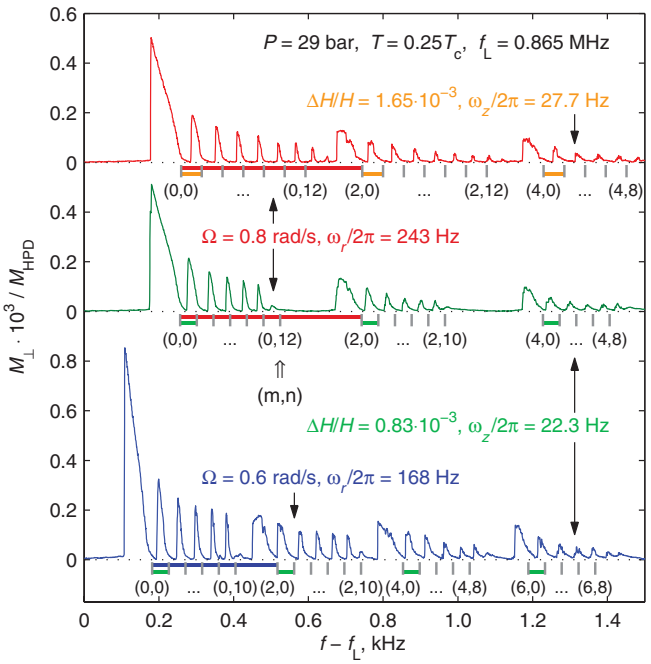

FIG. 4 (color). Formation of magnon condensates at different excited levels (m, n) of the magnetic trap in Fig. 1. When the frequency of the rf excitation field is swept down and crosses one of the levels (m, n) at f_{mn}, the magnon condensate starts to grow according to Eq. (7). Only modes with even m and n are excited. The three examples of measured spectra are for different values of rotation velocity Ω in the vortex-free state and for different depths $\Delta H/H$ of the axial field minimum in the trap. In the topmost case the depth of the field minimum is twice that of the two bottom examples. As a result, the smaller axial level spacing increases, as the axial oscillator frequency $\omega_z/2\pi$: 22 → 27 Hz, but the larger radial level spacing remains unchanged. Similarly, when Ω is increased from 0.6 rad/s (bottom spectrum) to 0.8 rad/s (two top most spectra), the radial level separation increases, as $\omega_r/2\pi$: 170 → 240 Hz. The equidistant vertical tick marks refer to the level positions in the absence of magnons and have been fitted to the harmonic trap relation in Eq. (4).

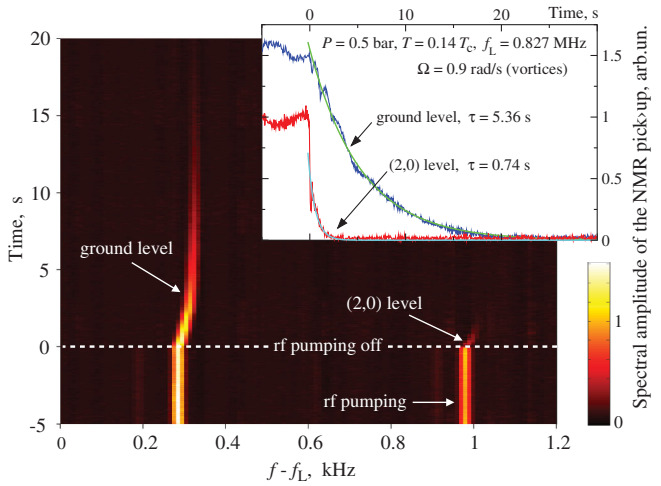

FIG. 5 (color). Decay of the magnon condensate, after rf pumping is switched off at $t = 0$. The amplitude of the Fourier transform of the signal from the NMR pick-up coil is shown in the main panel. Magnons are pumped to the (2, 0) level at $t < 0$, but the ground state is simultaneously populated owing to the decay of magnons from the excited state. At $t > 0$ both states decay [24] and the frequency of precession increases as the trap responds to the decreasing magnon population (Fig. 3). The *inset* shows the amplitudes of the two peaks and fits to exponential decay with time constant τ. The measurements have been performed at $0.14T_c$ in equilibrium rotation at 0.9 rad/s with rectilinear vortices.

ground state (0,0), which is filled by relaxation from the excited level. This type of quantum relaxation process for populating the ground state explains the off-resonance excitation at frequencies above the precession frequency ω_{00}, as observed in Ref. [14]. Excitation with white noise in a frequency band around ω_{00}, as reported in Refs. [15,16], is another manifestation of the process.

During the decay the magnon population follows closely the trajectory for the reverse process of Fig. 3. With decreasing temperature the relaxation rate in the ground state decreases rapidly—lifetimes ~15 min have been reported from observations at the lowest temperatures [17]. Our measurements in Fig. 5 on the decay from the excited state (2,0) show faster relaxation. However, the measured relaxation time is much longer than the dephasing time of the linear NMR response (about 10 ms in the same conditions). The long life time of free precession is a prominent experimental signature of these coherent condensate states. Although in practice coherent precession in an excited state is accompanied by coherent precession in the ground state, these are two independent phenomena, since their relaxation time scales are different and, moreover, when pumping at the ground-state frequency ω_{00} only the ground-state becomes occupied.

Conclusions.—Unlike ultracold atoms, coherently precessing magnon condensates in a magneto-textural trap with experimental control are subject to a potential which transforms with increasing magnon number from a harmonic well to a cylindrical box. For bosons this is the only demonstration so far of self-trapping, owing to the interaction of the growing number of particles with the confining quantum field. For fermions examples of self-formation of a boxlike trapping potential are the electron bubble in liquid helium [18] and the MIT bag model of a hadron [19], where the asymptotically free quarks are confined within a cavity in the pionic field.

In the magnon trap different excitation levels can be selectively populated with condensates, owing to an effective magnon-magnon interaction mediated by the orbital texture. These condensates provide important new possibilities for future measurements in the $T \to 0$ limit [10], particularly in terms of their relaxation properties. An urgent task is to determine whether the relaxation rate will reveal new information about surface [20] and

vortex-core bound states [21], in particular about their zero-energy modes with Majorana fermions, which are a characteristic of the topological insulator state of superfluid ^{3}He-B. So far large temperature-independent surface relaxation has been reported when the magnetic trap borders to a boundary [22], while we have preliminary observations of enhanced relaxation with increasing vortex number within the condensate. The proper understanding of these effects remains a task for the future.

Supported by the Academy of Finland, the EU-FP7 program (# 228464 Microkelvin), and by the CNRS-Russian Academy of Sciences collaboration (# N16569).

[1] Yu. M. Bunkov and G. E. Volovik, Phys. Rev. Lett. **98**, 265302 (2007).
[2] S. O. Demokritov, V. E. Demidov, O. Dzyapko, G. A. Melkov, A. A. Serga, B. Hillebrands, and A. N. Slavin, Nature (London) **443**, 430 (2006).
[3] J. Klaers, J. Schmitt, F. Vewinger, and M. Weitz, Nature (London) **468**, 545 (2010).
[4] F. Manni, K. G. Lagoudakis, T. C. H. Liew, R. André, and B. Deveaud-Plédran, Phys. Rev. Lett. **107**, 106401 (2011).
[5] Yu. M. Bunkov and G. E. Volovik, arXiv:1003.4889; J. Phys. Condens. Matter **22**, 164210 (2010).
[6] Yu. M. Bunkov, S. N. Fisher, A. M. Guénault, and G. R. Pickett, Phys. Rev. Lett. **69**, 3092 (1992).
[7] S. R. Coleman, Nucl. Phys. **B262**, 263 (1985).
[8] E. R. F. Ramos, E. A. L. Henn, J. A. Seman, M. A. Caracanhas, K. M. F. Magalhães, K. Helmerson, V. I. Yukalov, and V. S. Bagnato, Phys. Rev. A **78**, 063412 (2008).
[9] V. I. Yukalov, Phys. Part. Nucl. **42**, 460 (2011).
[10] V. B. Eltsov, R. de Graaf, M. Krusius, and D. E. Zmeev, J. Low Temp. Phys. **162**, 212 (2011).
[11] V. B. Eltsov, R. de Graaf, P. J. Heikkinen, J. J. Hosio, R. Hänninen and M. Krusius, J. Low Temp. Phys. **161**, 474 (2010).
[12] L. Pitaevskii and S. Stringari, *Bose-Einstein Condensation* (Clarendon Press, Oxford, UK, 2003).
[13] R. de Graaf, V. B. Eltsov, P. J. Heikkinen, J. J. Hosio, and M. Krusius, J. Low Temp. Phys. **163**, 238 (2011).
[14] D. J. Cousins, S. N. Fisher, A. I. Gregory, G. R. Pickett, and N. S. Shaw, Phys. Rev. Lett. **82**, 4484 (1999).
[15] S. N. Fisher, A. M Guénault, G. R Pickett, P. Skyba, Physica (Amsterdam) **329–333B**, 80 (2003).
[16] A. V. Chumak, G. A. Melkov, V. E. Demidov, O. Dzyapko, V. L. Safonov, and S. O. Demokritov, Phys. Rev. Lett. **102**, 187205 (2009).
[17] S. N. Fisher, A. M Guénault, A. J. Hale, G. R. Pickett, P. A. Reeves and G. Tvalashvili, J. Low Temp. Phys. **121**, 303 (2000).
[18] A. F. Borghesani, *Ions and Electrons in Liquid Helium* (Oxford University Press, Oxford, UK, 2007).
[19] A. Chodos, R. L. Jaffe, K. Johnson, C. B. Thorn, and V. F. Weisskopf, Phys. Rev. D **9**, 3471 (1974); **10**, 2599 (1974).
[20] Suk Bum Chung and Shou-Cheng Zhang, Phys. Rev. Lett. **103**, 235301 (2009).
[21] M. A. Silaev and G. E. Volovik, J. Low Temp. Phys. **161**, 460 (2010); M. A. Silaev, Phys. Rev. Lett. **108**, 045303 (2012).
[22] D. I. Bradley, D. O. Clubb, S. N. Fisher, A. M. Guénaugt, C. J. Matthews, G. R. Pickett, and P. Skyba, J. Low Temp. Phys. **134**, 351 (2004).
[23] Experimentally $M_\perp = \chi(T)H \int d^3r \sin\beta_M$ is convenient to normalize by means of the HPD where $M_{\mathrm{HPD}} = M_\perp|_{\beta_M=104^\circ}$, after correcting for the temperature difference.
[24] With two condensates in the trap during the decay of the excited-state condensate, one might expect Josephson coupling between the condensates [25], which would in the present case correspond to oscillations in the population of the excited state relative to that of the ground state. In Fig. 5 oscillations are not seen, since the FFT time window is longer than the expected period of the oscillations. With a narrower FFT window the signal-to-noise ratio decreases; it is not yet known if this or some more fundamental difficulty obscures a Josephson signal.
[25] K. G. Lagoudakis, B. Pietka, M. Wouters, R. André, and B. Deveaud-Plédran, Phys. Rev. Lett. **105**, 120403 (2010).